Available online at www.sciencedirect.com

ScienceDirect

IFAC Papers Online CONFERENCE PAPER ARCHIVE

IFAC-PapersOnLine 49-26 (2016) 213–218

Contractivity of a genetic circuit with internal feedback and cell-to-cell communication ⋆

E. Picó-Marco * **Y. Boada** * **J. Picó** * **A. Vignoni** **

* *I.U. de Automática e Informática Industrial (ai2), Universitat Politècnica de Valencia, 46022, Camino de Vera S/N, Valencia, Spain. (e-mail: {enpimar, yaboa,jpico}@upv.es)*

** *Center for Systems Biology Dresden and the Max Planck Institute of Molecular Cell Biology and Genetics, Pfotenhauer str. 108, 01307 Dresden, Germany. (e-mail: vignoni@mpi-cbg.de)*

Abstract: We consider a realistic model of the synthetic gene circuit combining cell-to-cell communication system via quorum sensing, and a synthetic repressible promoter implementing intracellular negative feedback control. The circuit has been shown to increase robustness with respect to both extrinsic and intrinsic noise elsewhere. As a first step towards an analytic analysis, in this paper we use contraction theory to perform a stability analysis. From it, we infer the components of the circuit most affecting the rate of contractivity, using biologically sensible values of the circuit parameters.

Keywords: Synthetic biology, Cell-to-cell communication, Differential stability, Contractivity

1. INTRODUCTION

Two key generic challenges of the bioprocess industries are developing efficient production systems for protein synthesis and expression, and the rational design and optimization of synthetic pathways for the synthesis of commodities. Heterologous protein synthesis starts by introducing an exogenous protein-coding gene in the cell, so that this produces the corresponding protein. Traditionally, for the design, optimization and control of bioprocesses, the population of microorganisms has been typically considered as an aggregate quantity characterized by averaged properties (Carlquist et al., 2012). Yet, it is a fact that even isogenic (i.e. with the same genetic content) microbial populations have certain degree of heterogeneity. Indeed, individual microorganisms, even if part of a clonal or isogenic population, may differ greatly in terms of genetic composition, physiology, biochemistry, or behavior (Elowitz et al., 2002; Toni and Tidor, 2013; Picó et al., 2015). In particular, the phenomenon of phenotypic noise is described as variation within an isogenic population due to fluctuations in gene expression of single cells (Toni and Tidor, 2013). This heterogeneity at the population level has been shown to be one of the causes of decrease in productivity when scaling-up to an industrial production bioprocess (Fernandes et al., 2011). Characterization and control of protein expression moments (mean and variance) across the cell population is, thus, a hot topic (Sánchez and Kondev, 2008; Weber and Buceta, 2011; Vignoni et al., 2013; Mélykúti et al., 2014; Oyarzu n et al., 2014) of relevance also for synthesis of commodities through synthetic pathways (Oyarzuun, 2011).

Dealing with the problems above requires both appropriate dynamic predictive models, and designing dynamic controls of the synthetic pathways and expression systems (Holtz and Keasling, 2010; Singh, 2011; Vignoni et al., 2013). An area of particular relevance is the design of collective cell behavior, whereby a prescribed population response results from the interaction between individual cells. A common approach to induce collective behavior is to use cell- to-cell communication mechanisms. These typically rely on the quorum sensing machinery from *V. fischeri*, and have been used for diverse purposes such as population synchronization (Nikolaev and Sontag, 2015), cell density-based control of gene expression (Williams et al., 2013), engineered cell social behavior Youk and Lim (2014), etc. The effect of cell-to-cell communication on noise regulation was also analyzed in (Tanouchi et al., 2008; Weber and Buceta, 2011; Boada et al., 2015). Following this line, in (Vignoni et al., 2013) we proposed a preliminary synthetic gene circuit aimed at controlling the mean and variance of protein expression across a cell population. The circuit uses both an intracellular negative feedback loop, and an external loop using quorum sensing as a means for cell-to-cell communication. Using a very simplified model we proved that the trajectories of the cell states converge to a closed region, wherein expressions for the mean and variance of the states could be obtained, using a linearised model, when variability in a key parameter of the circuit is present.

In this paper we consider a realistic model of the synthetic gene circuit. Analysis of stability of the circuit cannot be addressed using standard Lyapunov techniques, given the complexity of the model. Provided the system has a stable equilibrium point, a linearised model could be used to infer the effects of the circuit both on intrinsic and extrinsic noise, using an approach analogous to (Tanouchi et al., 2008; Vignoni et al., 2013). In this work, using contraction theory methods derived in (Russo and Di Bernardo, 2009; Russo et al., 2011; Margaliot et al., 2016), and realistic values for the parameters of the circuit, we derive the conditions under which the system has a stable equilibrium point.

⋆ This research was partially funded by grant FEDER-CICYT DPI2014-55276-C5-1-R. Yadira Boada thanks grant FPI/2013-3242 of the Universitat Politècnica de Valencia.

10.1016/j.ifacol.2016.12.128

The rest of the paper is organized as follows. In Section 2 we describe the gene synthetic circuit, and its mathematical model. In section 3 we perform the contraction analysis and, in section 4, its results for realistic values for the parameters of the circuit are derived. Finally, some conclusions and future work are drawn in the last section.

2. SYSTEM DESCRIPTION

Description of the synthetic gene network.

The proposed gene synthetic circuit, depicted in Fig. 1, combines two engineered gene networks previously implemented in *E. coli*: i) a cell-to-cell communication system via quorum sensing (QS) (Fuqua et al., 2001) using the autoinducer molecule acyl homoserine lactone AHL, and ii) a synthetic repressible promoter (Egland and Greenberg, 2000; Vignoni et al., 2013) implementing a negative feedback control over the concentration of the protein LuxI, the synthase that produces AHL. The ultimate goal of the circuit is to control the expression of an heterologous protein of interest which could be encoded in the same coding sequence as LuxI. This way, control of LuxI will be tantamount to that of the protein of interest except for its translation step. Notice transcription has been identified to be the protein expression step most affecting variability (Guimaraes et al., 2014)

The internal feedback loop aims at reducing the variability of LuxI at each individual cell. It consists of the gene *luxR* constitutively producing the protein LuxR. On the other hand, the protein LuxI synthesizes the autoinducer of the AHL inside each cell. Then, AHL binds to LuxR creating the monomer $(\mathrm{LuxR}\cdot\mathrm{AHL})$. In turn, two molecules dimerize producing $(\mathrm{LuxR}\cdot\mathrm{AHL})_2$. This complex is a transcription factor for the synthetic repressible promoter $\mathrm{P_{luxR}}$ promoter, controlling the expression of LuxI. Thus, the dimer $(\mathrm{LuxR}\cdot\mathrm{AHL})_2$ inhibits the transcription of the gene *luxI* downstream the $\mathrm{P_{luxR}}$ promoter. Hence, the circuit internal loop has a negative feedback loop between the intracellular AHL and LuxI.

The outer feedback loop accounts for the passive diffusion of AHL across the cell membrane to the culture medium, thus acting as communication signal within the population. This signal can be used to induce coordination in the cell population.

For the circuit above, we consider the main biochemical reactions involved: the genes regulated transcription and translation processes, the hetero- and homodimerization reactions involving the inducer, and diffusion of the inducer through the cell membrane. We simplify transcription of genes *luxI* and *luxR* by considering k_{mLuxI} and k_{mLuxR} as the effective irreversible transcription rates. Besides, α_{mLuxI} represents the basal transcription of the repressor $\mathrm{P_{luxR}}$. We also model translation as an irreversible reaction with an average transcription rate accounting for the fact that binding of ribosomes to the ribosome binding site (RBS) is indeed reversible, and several ribosomes may translate a single mRNA molecule simultaneously. Monomerization and dimerization are considered as reversible reactions. The diffusion process of the inducer across the cell membrane is modeled as a pseudo-reaction, where $\mathrm{V_c} = \mathrm{V_{cell}}/\mathrm{V_{ext}}$ is the ratio between the cell and the culture volume, that allows to quantify the number of intracellular AHL or extracellular $\mathrm{AHL_{ext}}$ molecules. With these simplifying assumptions in mind, the resulting set of reactions is shown in

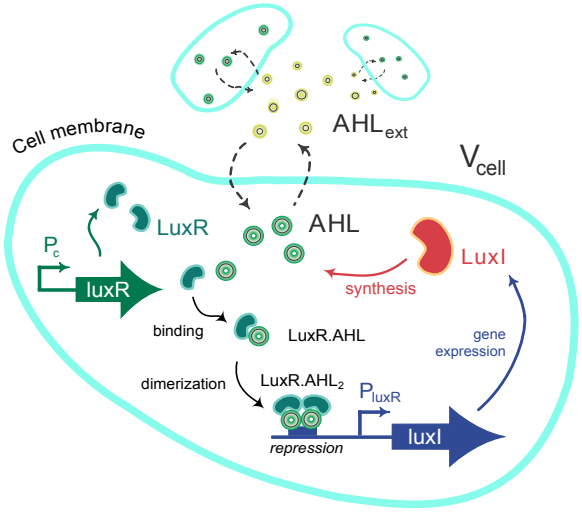

Fig. 1. Synthetic gene circuit.

(1). For convenience, we denote by DNA the free promoter of the gene *luxI*. The messenger RNAs of genes *luxI* and *luxR* are denoted as $\mathrm{mRNA_{luxI}}$ and $\mathrm{mRNA_{luxR}}$ respectively.

$$
\begin{aligned}
&\mathrm{DNA} \xrightarrow{k_{\mathrm{mLuxI}}} \mathrm{DNA} + \mathrm{mRNA_{luxI}}\\
&\xrightarrow{k_{\mathrm{mLuxR}}} \mathrm{mRNA_{luxR}}\\
&\mathrm{DNA(LuxR\cdot AHL)_2} \xrightarrow{\alpha_{\mathrm{mLuxI}} k_{\mathrm{mLuxI}}} \mathrm{DNA(LuxR\cdot AHL)_2} + \mathrm{mRNA_{luxI}}\\
&\mathrm{mRNA_{luxI}} \xrightarrow{k_{\mathrm{LuxI}}} \mathrm{mRNA_{luxI}} + \mathrm{LuxI}\\
&\mathrm{mRNA_{luxR}} \xrightarrow{k_{\mathrm{LuxR}}} \mathrm{mRNA_{luxR}} + \mathrm{LuxR}\\
&\mathrm{LuxI} \xrightarrow{k_A} \mathrm{AHL} + \mathrm{LuxI}\\
&\mathrm{LuxR} + \mathrm{AHL} \underset{k_1^-}{\overset{k_1^-/k_{d1}}{\rightleftarrows}} \mathrm{LuxR\cdot AHL}\\
&2(\mathrm{LuxR\cdot AHL}) \underset{k_2^-}{\overset{k_2^-/k_{d2}}{\rightleftarrows}} (\mathrm{LuxR\cdot AHL})_2\\
&(\mathrm{LuxR\cdot AHL})_2 + \mathrm{DNA} \underset{k_{lux}^-}{\overset{k_{lux}^-/k_{dlux}}{\rightleftarrows}} \mathrm{DNA(LuxR\cdot AHL)_2}\\
&\mathrm{AHL} \underset{\mathrm{DV_c}}{\overset{\mathrm{D}}{\rightleftarrows}} \mathrm{AHL_{ext}}\\
&\mathrm{AHL} \xrightarrow{d_A} \emptyset\\
&\mathrm{AHL_{ext}} \xrightarrow{d_{A_e}} \emptyset\\
&\mathrm{mRNA_{luxI}} \xrightarrow{dm_I} \emptyset\\
&\mathrm{mRNA_{luxR}} \xrightarrow{dm_R} \emptyset\\
&\mathrm{LuxI} \xrightarrow{d_I} \emptyset\\
&\mathrm{LuxR} \xrightarrow{d_R} \emptyset\\
&\mathrm{LuxR\cdot AHL} \xrightarrow{d_{RA}} \emptyset\\
&(\mathrm{LuxR\cdot AHL})_2 \xrightarrow{d_{RA_2}} \emptyset
\end{aligned}
\tag{1}
$$

Mathematical model.

The dynamical deterministic model corresponding to the biochemical reactions (1) can be obtained using the mass-action kinetics formalism (Chellaboina et al., 2009; Picó et al., 2015). Due to the constitutive expression of gene *luxR*, we can assume

Table 1. **Biochemical species for model** (2)**.**

State	Biochemical species	Name
n_1	Messenger RNA of *luxI*	mRNA_{luxI}
n_2	Messenger RNA of *luxR*	mRNA_{luxR}
n_3	Protein LuxI	LuxI
n_4	Protein LuxR	LuxR
n_5	Monomer	$(\mathrm{LuxR}\cdot\mathrm{AHL})$
n_6	Dimer	$(\mathrm{LuxR}\cdot\mathrm{AHL})_2$
n_7	Free promoter	DNA
n_8	Bound promoter	$\mathrm{DNA}(\mathrm{LuxR}\cdot\mathrm{AHL})_2$
n_9	Intracellular autoinducer	AHL
n_{10}	Extracellular autoinducer	$\mathrm{AHL}_{\mathrm{ext}}$

the number of molecules of protein LuxR is at steady state for practical purposes. Besides, the sum of the free (DNA) and bound ($\mathrm{DNA}(\mathrm{LuxR}\cdot\mathrm{AHL})_2$) promoter remains invariant, and equal to the gene copy number c_n. Moreover, the dimerization reaction is faster than the monomerization one, so the number of molecules of dimer, n_6, can be assumed to be at quasi-steady state. Thus, we obtain the reduced model (2):

$$
\begin{aligned}
\dot{n}_1^i &= k_{\mathrm{mLuxI}} c_n + k_{\mathrm{mLuxI}} \left(\alpha_{\mathrm{mLuxI}} - 1\right) n_8^i - d_{m_I} n_1^i \\
\dot{n}_3^i &= k_{\mathrm{LuxI}} n_1^i - d_I n_3^i \\
\dot{n}_4^i &= k_{\mathrm{LuxR}} \frac{k_{\mathrm{mLuxR}} c_n}{d_{m_R}} + k_1^- n_5^i - d_R n_4^i - \frac{k_1^-}{k_{d1}} n_9^i n_4^i \\
\dot{n}_5^i &= 2k_2^- n_6^i + \frac{k_1^-}{k_{d1}} n_9^i n_4^i - \left(k_1^- + d_{RA} + 2\frac{k_2^-}{k_{d2}} n_5^i\right) n_5^i \\
n_6^i &= \frac{k_{\mathrm{lux}}^- n_8^i + \frac{k_2^-}{k_{d2}} (n_5^i)^2}{k_2^- + d_{RA_2} + \frac{k_{\mathrm{lux}}^-}{k_{\mathrm{dlux}}} \left(c_n - n_8^i\right)} \approx \frac{k_{\mathrm{lux}}^- n_8^i + \frac{k_2^-}{k_{d2}} (n_5^i)^2}{k_2^- + d_{RA_2}} \\
\dot{n}_8^i &= -k_{\mathrm{lux}}^- n_8^i + \frac{k_{\mathrm{lux}}^-}{k_{\mathrm{dlux}}} n_6^i \left(c_n - n_8^i\right) \\
\dot{n}_9^i &= D\left(\frac{V_{\mathrm{cell}}}{V_{\mathrm{ext}}} n_{10} - n_9^i\right) - \left(\frac{k_1^-}{k_{d1}} n_4^i + d_A\right) n_9^i \\
&\quad + k_1^- n_5^i + k_A n_3^i \\
\dot{n}_{10} &= D\left(-N\frac{V_{\mathrm{cell}}}{V_{\mathrm{ext}}} n_{10} + \sum_{i=1}^{N} n_9^i\right) - d_{A_e} n_{10}
\end{aligned}
\tag{2}
$$

where the first nine are the states for each *i*-th cell in a population of N cells. The 10th state corresponds to the extracellular autoinducer molecule. The states are described in Table 1. Notice the free promoter n_7 is not used, as $n_7 + n_8 = c_n$ was used as invariant for the model reduction.

A description of the parameters in model (2), and realistic values for them is shown in Table 2.

3. CONTRACTION ANALYSIS

A system $\dot{x} = f(x,t)$ is contractive within a region of the state space if the jacobian $\partial f/\partial x$ is uniformly negative in that region. Inttuitively it means within the contractive region trajectories approach to each other and initial conditions are forgotten. This result can be generalized using riemannian metrics (Lohmiller and Slotine, 1998). A sufficient, and much easier to prove, condition is given in (Russo and Di Bernardo, 2009; Russo et al., 2011) and we use it to infer if the system (2), considering N cells, is contractive. First we must derive

Table 2. **Parameters in model** (2)**.**

Parameter	Description	Value	Reference
c_n	Plasmid copy number	17 plasmids/cell	plasmid PBR322
k_{mLuxR}	Transcription rate*luxR*	4.4 min^{-1}	estimated
$\mathrm{dm_R}$	Degradation rate $\mathrm{mRNA_{LuxR}}$	0.17 min^{-1}	Milo and Phillips (2016)
k_{LuxR}	Translation rate *luxR*	55 min^{-1}	estimated
$\mathrm{d_R}$	Degradation rate of LuxR	0.1745 min^{-1}	tagged LuxR
k_{mLuxI}	Transcription rate of *luxI*	2.5 min^{-1}	estimated
α_{mLuxI}	Basal transcription factor for *luxI*	0.01	Weber et al. (2013)
$\mathrm{dm_I}$	Degradation rate of $\mathrm{mRNA_{LuxI}}$	0.3624 min^{-1}	Roberts et al. (2006)
k_{LuxI}	Translation rate of LuxI	6.94 min^{-1}	Boada et al. (2015)
$\mathrm{d_I}$	Degradation rate of LuxI	0.0174min^{-1}	cell half-life 40 min
$\mathrm{k_1^-}$	Dissociation rate of LuxR to AHL	10 min^{-1}	Weber et al. (2013)
$\mathrm{k_{d1}}$	Dissociation LuxR /AHL	150 molecules	Urbanowski et al. (2004)
d_{RA}	Degradation rate of $(\mathrm{LuxR}\cdot\mathrm{AHL})$	0.0174 min^{-1}	cell half-life 40 min
k_2^-	Dissociation rate of $(\mathrm{LuxR}\cdot\mathrm{AHL})_2$	1 min^{-1}	Weber et al. (2013)
k_{d2}	Dissociation $(\mathrm{LuxR}\cdot\mathrm{AHL})_2$	35 molecules	fitted
d_{RA_2}	Degradation rate of $(\mathrm{LuxR}\cdot\mathrm{AHL})_2$	0.0174 min^{-1}	cell half-life 40 min
$\mathrm{d_A}$	Degradation rate internal AHL	0.0164 min^{-1}	Kaufmann et al. (2005)
$\mathrm{d}_{\mathrm{A_e}}$	Degradation rate external AHL	0.004 min^{-1}	Kaufmann et al. (2005)
D	Diffusion rate AHL /cell membrane	2 min^{-1}	Kaplan and Greenberg (1985)
$\mathrm{k_A}$	Synthesis rate of AHL by LuxI	0.04 min^{-1}	Garcia-Ojalvo et al. (2004)
$\mathrm{k_{lux}}$	Dissociation rate $(\mathrm{LuxR}\cdot\mathrm{AHL})_2/\mathrm{P_{luxR}}$	10 min^{-1}	Weber et al. (2013)
$\mathrm{k_{dlux}}$	Dissociation $(\mathrm{LuxR}\cdot\mathrm{AHL})_2$/promoter	140 molecules	fitted

the Jacobian matrix. Notice that given the structure of (2), the Jacobian for N cells will have the blocks structure (3):

$$
J_N = \begin{bmatrix}
J_c^1 & \mathbf{0}_{6\times 6} & \cdots & \mathbf{0}_{5\times 1} \\
 & & & D\frac{V_{\mathrm{cell}}}{V_{\mathrm{ext}}} \\
\mathbf{0}_{6\times 6} & J_c^2 & \cdots & \mathbf{0}_{5\times 1} \\
 & & & D\frac{V_{\mathrm{cell}}}{V_{\mathrm{ext}}} \\
\vdots & \vdots & \ddots & \vdots \\
\mathbf{0}_{1\times 5}\ D & \mathbf{0}_{1\times 5}\ D & \cdots & -ND\frac{V_{\mathrm{cell}}}{V_{\mathrm{ext}}} - d_{A_e}
\end{bmatrix}
\tag{3}
$$

where each subblock J_c^i, for $i = 1, \ldots, N$ is the Jacobian w.r.t. the states n_1 to n_9 for each cell. The detailed expression for J_c^i can be found in table 3. From the Jacobian, we obtain an adjacency matrix corresponding to an undirected associated graph to the system Jacobian. The graph contains as many nodes as states. Two nodes (p, q) are connected if either $J_N(p,q) \neq 0$ or $J_N(q,p) \neq 0$. The resulting adjacency matrix takes the form (3)

$$
A_N = \begin{bmatrix}
A_c^1 & \mathbf{0}_{6\times 6} & \cdots & \mathbf{0}_{5\times 1} \\
 & & & 1 \\
\mathbf{0}_{6\times 6} & A_c^2 & \cdots & \mathbf{0}_{5\times 1} \\
 & & & 1 \\
\vdots & \vdots & \ddots & \vdots \\
\mathbf{0}_{1\times 5}\ 1 & \mathbf{0}_{1\times 5}\ 1 & \cdots & 0
\end{bmatrix}
\tag{4}
$$

where, again, each sub-block A_c^i, for $i = 1, \ldots, N$ is the adjacency matrix w.r.t. the states n_1 to n_9 for each cell:

$$
A_c^i = \begin{bmatrix}
0 & 1 & 0 & 0 & 1 & 0 \\
1 & 0 & 0 & 0 & 0 & 1 \\
0 & 0 & 0 & 1 & 0 & 1 \\
0 & 0 & 1 & 0 & 1 & 1 \\
1 & 0 & 0 & 1 & 0 & 0 \\
0 & 1 & 1 & 1 & 0 & 0
\end{bmatrix}
\tag{5}
$$

Contractiveness of the synthetic network is guaranteed if the next conditions are fulfilled:

(1) All diagonal elements of the Jacobian matrix J_N are uniformly negative.
(2) Given, for any pair (p, q), the computed values $\alpha_{p,q} = \frac{|J_{N,p,q}(t,\mathbf{n})|}{|J_{N,p,p}(t,\mathbf{n})|}(m - n_{0p} - 1)$, the conditions $\alpha_{p,q}\alpha_{q,p} \leq 1$ must be met uniformly in t.
(3) The values of $\alpha_{p,q}$ determine the directions in the associated graph to the adjacency matrix (3) (see (Russo et al., 2011) for details). No closed cycles can exist in the directed graph.

$$J_c^i = \begin{bmatrix} -d_{m_I} & 0 & 0 & 0 & k_{\mathrm{mLuxI}}\,(\alpha_{\mathrm{mLuxI}}-1) & 0 \\ k_{\mathrm{LuxI}} & -d_I & 0 & 0 & 0 & 0 \\ 0 & 0 & -d_R - \frac{k_1^-}{k_{d1}} n_9^i & k_1^- & 0 & -\frac{k_1^-}{k_{d1}} n_4^i \\ 0 & 0 & \frac{k_1^-}{k_{d1}} n_9^i & -k_1^- - d_{RA} - 4\frac{d_{RA_2}}{d_{RA_2}+k_2^-}\frac{k_2^-}{k_{d2}} n_5^i & 2k_2^- \frac{k_{\mathrm{lux}}^-}{d_{RA_2}+k_2^-} & \frac{k_1^-}{k_{d1}} n_4^i \\ 0 & 0 & 0 & \frac{k_{\mathrm{lux}}^-}{k_{\mathrm{dlux}}} \frac{2\frac{k_2^-}{k_{d2}} n_5}{d_{RA_2}+k_2^-}\left(c_n - n_8^i\right) & -k_{\mathrm{lux}}^- - \frac{k_{\mathrm{lux}}^-}{k_{\mathrm{dlux}}}\frac{k_{\mathrm{lux}}^-}{d_{RA_2}+k_2^-}\left(2n_8^i - c_n + \frac{k_2^-}{k_{d2}}\frac{n_5^{2,i}}{k_{\mathrm{lux}}^-}\right) & 0 \\ 0 & k_A & -\frac{k_1^-}{k_{d1}} n_9^i & 0 & 0 & -D - \frac{k_1^-}{k_{d1}} n_4^i - d_A \end{bmatrix}$$

Table 3. Jacobian J_c^i

Table 4. **Expressions for $\alpha_{p,q}$.**

$\alpha_{1,2} = 0$	$\alpha_{2,1} = \frac{k_{\mathrm{LuxI}}}{d_I}$
$\alpha_{1,5} = \frac{k_{\mathrm{mLuxI}}\lvert\alpha_{\mathrm{mLuxI}}-1\rvert}{d_{mI}}$	$\alpha_{5,1} = 0$
$\alpha_{2,6} = 0$	$\alpha_{6,2} = \frac{3k_A}{D+d_A+\frac{k_1^-}{k_{d1}} n_4^i}$
$\alpha_{3,4} = \frac{k_1^-}{d_R+\frac{k_1^-}{k_{d1}} n_9^i}$	$\alpha_{4,3} = \frac{2\frac{k_1^-}{k_{d1}} n_9^i}{k_1^- + d_{RA} + \frac{4\frac{d_{RA_2}}{k_{d2}}\frac{k_2^-}{k_{d2}} n_5^i}{k_2^- + d_{RA_2}}}$
$\alpha_{3,6} = \frac{\frac{k_1^-}{k_{d1}} n_4^i}{d_R+\frac{k_1^-}{k_{d1}} n_9^i}$	$\alpha_{6,3} = \frac{3\frac{k_1^-}{k_{d1}} n_9^i}{D+d_A+\frac{k_1^-}{k_{d1}} n_4^i}$
$\alpha_{4,6} = \frac{2\frac{k_1^-}{k_{d1}} n_4^i}{k_1^- + d_{RA} + \frac{4\frac{d_{RA_2}}{k_{d2}}\frac{k_2^-}{k_{d2}} n_5^i}{k_2^- + d_{RA_2}}}$	$\alpha_{6,4} = 0$
$\alpha_{4,5} = \frac{4k_2^-\frac{k_{\mathrm{lux}}^-}{k_2^- + d_{RA_2}}}{k_1^- + d_{RA} + \frac{4\frac{d_{RA_2}}{k_{d2}}\frac{k_2^-}{k_{d2}} n_5^i}{k_2^- + d_{RA_2}}}$	$\alpha_{5,4} = \frac{\frac{2\frac{k_2^-}{k_{d2}} n_5^i}{d_{RA_2}+k_2^-}(c_n - n_8^i)}{k_{\mathrm{dlux}} + \frac{k_{\mathrm{lux}}^-}{d_{RA_2}+k_2^-}\left\lvert\frac{k_2^- n_5^{2,i}}{k_{d2} k_{\mathrm{lux}}^-} + 2n_8^i - c_n\right\rvert}$
$\alpha_{6,7} = \frac{3D\frac{V_{\mathrm{cell}}}{V_{\mathrm{ext}}}}{d_A + D + \frac{k_1^-}{k_{d1}} n_4^i}$	$\alpha_{7,6} = \frac{(N-1)D}{ND\frac{V_{\mathrm{cell}}}{V_{\mathrm{ext}}} + d_{A_e}}$

The first condition is clearly fulfilled, taking into account that $n_j^i \geq 0\ \forall i = 1 \cdots N, j = 1 \cdots 8$, and the number of occupied promoters in each cell fulfills $n_8^i \leq c_n$.

On the other hand, notice that for any row and column p, q of the Jacobian J_N we have that $\alpha_{p,q} = 0$ for any pair (p, q) such that $p \in J_c^i$ and $q \in J_c^j$ for $i \neq j$. Therefore, the only terms $\alpha_{p,q}$ that matter are the ones corresponding to the subgraphs associated to the interactions within each cell, and between each cell and the external AHL_e molecules. Therefore, it suffices considering the Jacobian submatrix J_c^i given in equation (3). Notice also that the only values of $\alpha_{p,q}$ that must be computed from the cell Jacobian sub-matrix J_c^i are the ones for which $A_c(p, q) = 1$. This results in table 4

Since $V_{\mathrm{cell}} \ll V_{\mathrm{ext}}$ notice that $\alpha_{6,7} < 1$ for any $n_4^i \geq 0$, and $\alpha_{7,6} \geq 1$ provided

$$N \geq 1 + \frac{d_{A_e}}{D} \tag{6}$$

where we approximated $\frac{V_{\mathrm{ext}} - V_{\mathrm{cell}}}{V_{\mathrm{ext}}} \approx 1$. Using the typical values of d_{A_e} and D given in table 2, we see that $\alpha_{7,6} > 1$ for $N \geq 2$, i.e. whenever we have two or more cells.

4. RESULTS

Using the parameter values shown in Table 2 we simulated 100 cells starting from different initial conditions. After a short transient, the values of the products $\alpha_{p,q}\alpha_{q,p} \leq 1$, as shown in figure 2.

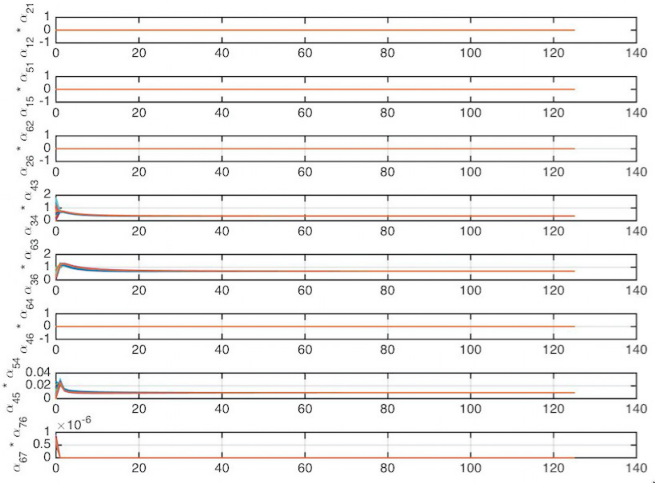

Fig. 2. Time evolution of the products $\alpha_{p,q}\alpha_{q,p}$.

Figure 3 shows the graph associated to the synthetic gene network for the values of α obtained for the nominal values in table 2. It can be observed that no closed loop exists.

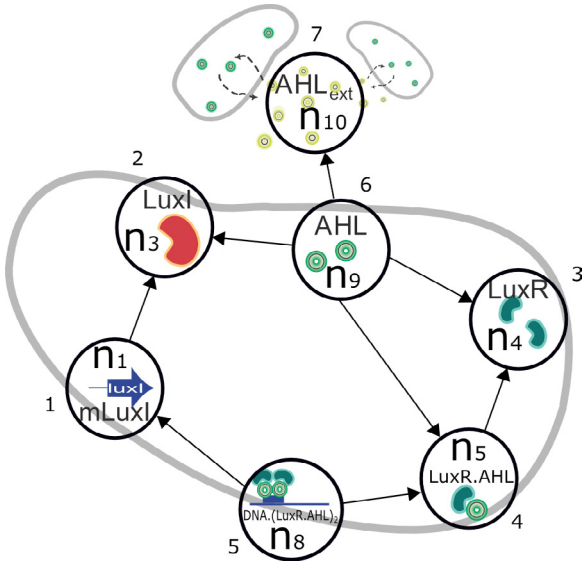

Fig. 3. Graph associated to the synthetic gene circuit.

Under this conditions, the genetic network is contractive. Thus, all trajectories starting from different initial conditions will converge to a common one. Provided the system has an equilibrium

within the state space region where it is contractive, the trajectories will converge to it. In case the network is composed of identical cells with different initial conditions, all will converge to a common state, as seen in figure 4.

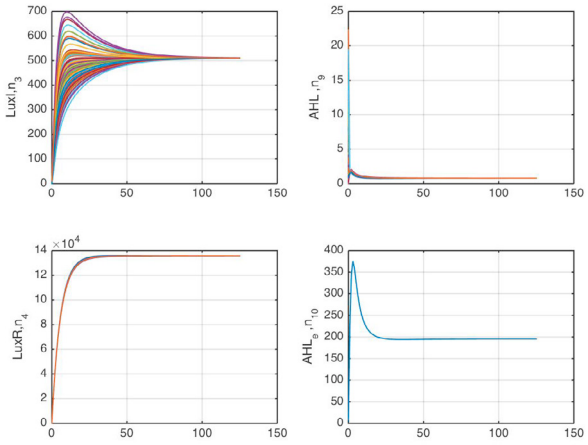

Fig. 4. Time evolution of $LuxI$, $LuxR$, AHL_i and AHL_e for a network composed of $N = 100$ cells, each one with different initial state.

5. DISCUSSION AND CONCLUSIONS

From table 4 and the results in figure 2 it can be seen that the $\alpha_{p,q}\alpha_{q,p}$ products that are critical to ensure sufficient conditions for attractiveness of the circuit are $\alpha_{36}\alpha_{63}$ and, to a minor extent, $\alpha_{34}\alpha_{43}$. This products are associated to the edges between the species n_4-n_9 ($AHL_i - LuxR$) and n_4-n_5 ($LuxR - (LuxR \cdot AHL_i)$) respectively (see figure 3). Thus, they are related to the formation of the monomer $LuxR \cdot AHL_i$. Thus, it seems that the relative abundances of intracellular AHL_i, $LuxR$, and the monomer $LuxR \cdot AHL_i$) are critical to ensure contractivity of the circuit. Indeed, the mentioned α-products are:

$$\alpha_{3,4}\alpha_{4,3} = 2\frac{\frac{k_1^-}{k_{d1}}n_9^i}{d_R + \frac{k_1^-}{k_{d1}}n_9^i}\frac{k_1^-}{k_1^- + d_{RA} + \frac{4\frac{d_{RA_2}k_2^-}{k_{d2}}n_5^i}{k_2^- + d_{RA_2}}}$$
$$\alpha_{3,6}\alpha_{6,3} = 3\frac{\frac{k_1^-}{k_{d1}}n_9^i}{d_R + \frac{k_1^-}{k_{d1}}n_9^i}\frac{\frac{k_1^-}{k_{d1}}n_4^i}{D + d_A + \frac{k_1^-}{k_{d1}}n_4^i} \quad (7)$$

For biologically realistic values of the circuit parameters, the amount of free intracellular AHL_i (n_9^i) is very low (order of magnitude of 1), while the amount of $LuxR$ (n_4^i) is several orders of magnitude higher. This implies, that the key term to achieve $\alpha_{3,6}\alpha_{6,3} \leq 1$ is the dynamics of $LuxR$. A large degradation rate d_R of $LuxR$ will contribute to lower values of $\alpha_{3,6}\alpha_{6,3}$. The same holds for $\alpha_{3,4}\alpha_{4,3}$. This result is consistent with the findings in (Tanouchi et al., 2008; Boada et al., 2015), where it was shown that a fast turnover of $LuxR$ contributes to higher robustness with respect to both extrinsic and intrinsic noise respectively. Indeed, higher contraction rates protect from noise (Tabareau et al., 2010). Yet, this effect will depend on the amount of free AHL_i, which depends on how much monomer $LuxR \cdot AHL_i$ forms. This can be regulated by means of the RBS strength $kLuxR$. The lower the strength, the more free AHL_i in the cell. Thus, higher values of $\alpha_{3,6}\alpha_{6,3}$ will be obtained, as seen in figure 5. Notice for weak low values of $kLuxR$, condition $\alpha_{3,6}\alpha_{6,3} \leq 1$ does not hold. This justifies the common approach of using strong constitutive promoters and ribosome binding sites for $LuxR$, so it is in excess. Notice also that as $kLuxR$ increases, the transient required to ensure $\alpha_{3,6}\alpha_{6,3} \leq 1$ becomes shorter. This is important, as allowing small transients does not destroy the important asymptotic properties of contractive systems like convergence to a unique equilibrium point (Margaliot et al., 2016).

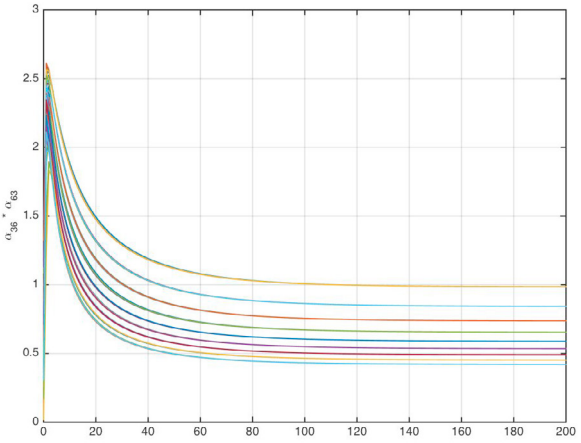

Fig. 5. Time evolution of $\alpha_{3,6}\alpha_{6,3}$ as a function of $kLuxR$. The values of $kLuxR$ vary from $kLuxR = 20$ to $kLuxR = 55$. These values roughly correspond to expression of luxR (Bba_C0062) under the RBS of different strength, assuming translation rates $[2.4, 4.8]\text{min}^{-1}/\text{Ribosome}$, 750 bps length for LuxR, and ribosomes distributed approximately each 65 nucleotides. The value of $\alpha_{3,6}\alpha_{6,3}$ decreases as $kLuxR$ increases.

In conclusion, we have ensured that the system is contractive in a region where it has an equilibrium point. Therefore, this equilibrium point is, locally, an asymptotic stable one. This justifies the possibility of linearising the system around the equilibrium point, and use the linearised model to analyze the behavior of the genetic circuit with respect to extrinsic noise, using an approach similar to (Tanouchi et al., 2008; Vignoni et al., 2013). This analysis will give analytic clues on the paper played by cell-to-cell communication. Indeed, diffusion of AHL across the cell membrane, and the density of the cell population, affects the equilibrium value of the intracellular AHL_i, thus affecting the rate of contraction. A preliminary computational analysis has shown that the cell-to-cell communication effectively contributes to decrease the effect of intrinsic noise on $LuxI$. The analysis with respect to extrinsic noise is computationally expensive. Thus an analytic approach, even if approximated, will be of great use.

REFERENCES

Boada, Y., Vignoni, A., Navarro, J.L., and Picó, J. (2015). Improvement of a cle stochastic simulation of gene synthetic network with quorum sensing and feedback in a cell population. In *2015 European Control Conference (ECC)*.

Carlquist, M., Fernandes, R.L., Helmark, S., Heins, A.L.L., Lundin, L., Sorensen, S.J., Gernaey, K.V., and Lantz, A.E.

(2012). Physiological heterogeneities in microbial populations and implications for physical stress tolerance. *Microb Cell Fact*, 11, 94. doi:10.1186/1475-2859-11-94.

Chellaboina, V., Bhat, S., Haddad, W., and Bernstein, D. (2009). Modeling and analysis of mass-action kinetics. *IEEE Control Systems Magazine*, 29(4), 60–78. doi:10.1109/mcs.2009.932926.

Egland, K.A. and Greenberg, E.P. (2000). Conversion of the vibrio fischeri transcriptional activator, LuxR, to a repressor. *Journal of Bacteriology*, 182(3), 805–811.

Elowitz, M.B., Levine, A.J., Siggia, E.D., and Swain, P.S. (2002). Stochastic gene expression in a single cell. *Science*, 297(5584), 1183–6. doi:10.1126/science.1070919.

Fernandes, R.L., Nierychlo, M., Lundin, L., Pedersen, A.E., Puentes Tellez, P.E., Dutta, A., Carlquist, M., Bolic, A., Schäpper, D., Brunetti, A.C., Helmark, S., Heins, A.L.L., Jensen, A.D., Nopens, I., Rottwitt, K., Szita, N., van Elsas, J.D., Nielsen, P.H., Martinussen, J., Sorensen, S.J., Lantz, A.E., and Gernaey, K.V. (2011). Experimental methods and modeling techniques for description of cell population heterogeneity. *Biotechnol Adv*, 29(6), 575–99. doi:10.1016/j.biotechadv.2011.03.007.

Fuqua, C., Parsek, M., and Greenberg, E. (2001). Regulation of gene expression by cell-to-cell communication: acyl-homoserine lactone quorum sensing. *Annual review of genetics*, 35(1), 439–468.

Garcia-Ojalvo, J., Elowitz, M.B., and Strogatz, S.H. (2004). Modeling a synthetic multicellular clock: repressilators coupled by quorum sensing. *Proceedings of the National Academy of Sciences of the United States of America*, 101(30), 10955–10960.

Guimaraes, J.C., Rocha, M., and Arkin, A.P. (2014). Transcript level and sequence determinants of protein abundance and noise in escherichia coli. *Nucleic Acids Res*, 42(8), 4791–9. doi:10.1093/nar/gku126.

Holtz, W.J. and Keasling, J.D. (2010). Engineering static and dynamic control of synthetic pathways. *Cell*, 140(1), 19–23. doi:10.1016/j.cell.2009.12.029.

Kaplan, H. and Greenberg, E. (1985). Diffusion of autoinducer is involved in regulation of the vibrio fischeri luminescence system. *Journal of Bacteriology*, 163(3), 1210–1214.

Kaufmann, G.F., Sartorio, R., Lee, S.H., Rogers, C.J., Meijler, M.M., Moss, J.A., Clapham, B., Brogan, A.P., Dickerson, T.J., and Janda, K.D. (2005). Revisiting quorum sensing: discovery of additional chemical and biological functions for 3-oxo-n-acylhomoserine lactones. *Proceedings of the National Academy of Sciences of the United States of America*, 102(2), 309–314.

Lohmiller, W. and Slotine, J. (1998). On contraction analysis for nonlinear systems. *Automatica*, 36(6).

Margaliot, M., Sontag, E.D., and Tuller, T. (2016). Contraction after small transients. *Automatica*, 67, 178–184. doi:10.1016/j.automatica.2016.01.018.

Mélykúti, B., Hespanha, J.a.P., and Khammash, M. (2014). Equilibrium distributions of simple biochemical reaction systems for time-scale separation in stochastic reaction networks. *J R Soc Interface*, 11(97), 20140054. doi:10.1098/rsif.2014.0054.

Milo, R. and Phillips, R. (2016). *Cell Biology by the Numbers*. Garland.

Nikolaev, E. and Sontag, E. (2015). Quorum-sensing synchronization of synthetic toggle switches: A design based on monotone dynamical systems theory. *bioRxiv*, 024810.

Oyarzún, D.A. (2011). Optimal control of metabolic networks with saturable enzyme kinetics. *IET Syst Biol*, 5(2), 110–9. doi:10.1049/iet-syb.2010.0044.

Oyarzún, D.A., Lugagne, J.B..B., and Stan, G.B.V..B.V. (2014). Noise propagation in synthetic gene circuits for metabolic control. *ACS synthetic biology*, 4(2), 116–125.

Picó, J., Vignoni, A., Picó-Marco, E., and Boada, Y. (2015). Modelling biochemical systems: from mass action ki-netics to linear noise approximation. *Revista Iberoamericana de Automática e Informática Industrial RIAI*, 12(3), 241–252. doi:10.1016/j.riai.2015.06.001.

Roberts, C., Anderson, K.L., Murphy, E., Projan, S.J., Mounts, W., Hurlburt, B., Smeltzer, M., Overbeek, R., Disz, T., and Dunman, P.M. (2006). Characterizing the effect of the staphylococcus aureus virulence factor regulator, sara, on log-phase mrna half-lives. *Journal of bacteriology*, 188(7), 2593–2603.

Russo, G. and Di Bernardo, M. (2009). An algorithm for the construction of synthetic self synchronizing biological circuits. In *ISCAS*, 305–308.

Russo, G., di Bernardo, M., and Slotine, J.J.E. (2011). A graphical approach to prove contraction of nonlinear circuits and systems. *IEEE Trans. Circuits Syst. I*, 58(2), 336–348. doi:10.1109/tcsi.2010.2071810.

Sánchez, A. and Kondev, J. (2008). Transcriptional control of noise in gene expression. *Proceedings of the National Academy of Sciences*, 105(13), 5081–5086.

Singh, A. (2011). Negative feedback through mrna provides the best control of gene-expression noise. *NanoBioscience, IEEE Transactions on*, 10(3), 194–200.

Tabareau, N., Slotine, J.J.J., and Pham, Q.C.C. (2010). How synchronization protects from noise. *PLoS Comput Biol*, 6(1), e1000637. doi:10.1371/journal.pcbi.1000637.

Tanouchi, Y., Tu, D., Kim, J., and You, L. (2008). Noise reduction by diffusional dissipation in a minimal quorum sensing motif. *PLoS Comput Biol*, 4(8), e1000167. doi:10.1371/journal.pcbi.1000167.

Toni, T. and Tidor, B. (2013). Combined model of intrinsic and extrinsic variability for computational network design with application to synthetic biology. *PLoS Comput Biol*, 9(3), e1002960. doi:10.1371/journal.pcbi.1002960.

Urbanowski, M.L., Lostroh, C.P., and Greenberg, E.P. (2004). Reversible acyl-homoserine lactone binding to purified vibrio fischeri luxr protein. *Journal of Bacteriology*, 186(3), 631–637. doi:10.1128/jb.186.3.631-637.2004.

Vignoni, A., Oyarzún, D.A., Picó, J., and Stan, G.B. (2013). Control of protein concentrations in heterogeneous cell populations. In *2013 European Control Conference (ECC)*.

Weber, M. and Buceta, J. (2011). Noise regulation by quorum sensing in low mrna copy number systems. *BMC Syst Biol*, 5, 11. doi:10.1186/1752-0509-5-11.

Weber, M., Buceta, J., et al. (2013). Dynamics of the quorum sensing switch: stochastic and non-stationary effects. *BMC systems biology*, 7(1), 6.

Williams, T.C., Nielsen, L.K., and Vickers, C.E. (2013). Engineered quorum sensing using pheromone-mediated cell-to-cell communication in saccharomyces cerevisiae. *ACS synthetic biology*, 2(3), 136–149.

Youk, H. and Lim, W.A..A. (2014). Secreting and sensing the same molecule allows cells to achieve versatile social behaviors. *Science*, 343(6171), 1242782. doi:10.1126/science.1242782.